Fall 2012

Intracellular Expression of an Ice Nucleation Protein Reduces Cryoinjury in Insect Cells

Avril M. Harder
Eastern Illinois University

Intracellular Expression of an Ice Nucleation Protein Reduces Cryoinjury in Insect Cells

by

Avril M. Harder

HONORS THESIS

SUBMITTED IN PARTIAL FULFILLMENT OF THE REQUIREMENTS FOR THE DEGREE OF

BACHELOR OF SCIENCE IN BIOLOGICAL SCIENCES WITH HONORS

AT EASTERN ILLINOIS UNIVERSITY

CHARLESTON, ILLINOIS

December 2012

I hereby recommend that this Honors Thesis be accepted as fulfilling this part of the undergraduate degree cited above:

Thesis Director	Date
Honors Program Director	Date

ABSTRACT

Exposure of insect cells to subzero temperatures typically leads to cell membrane disruption and lethal intracellular ice formation. This study seeks to examine the cryoprotective value of trangenically expressing a bacterial ice nucleation protein (INP) in *Spodoptera frugiperda* (Sf-21) cells. The bacterium *Pseudomonas syringae* naturally produces a membrane-bound INP (inaZ), capable of structuring water and initiating ice formation at temperatures as high as -2 °C. I hypothesized that intracellular expression of an altered form of inaZ (*Ps*INP) in Sf-21 cells will mediate highly regulated ice nucleation when cells are cooled to -80 °C in a slow, controlled manner, and that cells expressing *Ps*INP (Sf-21-*Ps*INP) will maintain cell membrane integrity in greater proportions than wildtype cells (Sf-21-WT). Following one freeze-thaw cycle, 60% of Sf-21-WT cell membranes remained intact, while 72% of Sf-21-*Ps*INP cells maintained membrane integrity. This difference is statistically significant, and suggests that *Ps*INP expression helps to prevent cryoinjury during freezing, and positively impacts cell viability following thawing.

ACKNOWLEDGMENTS

I would like to express my deep gratitude to Dr. Michael Menze for his invaluable guidance and advice. He has provided me with a wonderful introduction to the world of cell physiology research, and will be forever grateful for the opportunity to conduct my undergraduate project in his lab. I would also like to thank our collaborator, Dr. Nilay Chakraborty, for his contributions and for providing me with an engineer's perspective on this study. Finally, I extend my appreciation to the EIU Biological Sciences faculty and to the Honors College, for supporting undergraduate research, and for providing a productive learning environment.

TABLE OF CONTENTS

INTRODUCTION

Under certain conditions some bacteria synthesize specific proteins that serve as nucleation centers for ice crystals (Gurian-Sherman and Lindow, 1993). These microorganisms present ice nucleation proteins (INPs) on the cell surface and efficiently catalyze ice formation at temperatures as warm as -2 °C (Gurian-Sherman and Lindow, 1993). First identified and isolated by Wolber et al. the product of the highly repetitive gene sequence *inaZ* is a membrane-bound protein (*Ps*INP) expressed by the bacterium *Pseudomonas syringae*; this protein provides a molecular foundation for the structuring of water molecules (Wolber et al., 1986). A virtually ubiquitous epiphytic pathogen, P. *syringae* induces frost damage in sensitive plant tissues at temperatures around -5 °C. Two main hypotheses about the functions of INPs have been postulated: a) to grant the bacterium access to nutrients in plant tissue and b) to provide a means of dispersal via the water cycle (Lindow et al., 1982; Morris et al., 2007; Morris et al., 2008). Furthermore, increasing proficiency of a particular strain at encouraging ice formation directly correlates to amplified virulence (Morris et al., 2010). Commercially important aspects include ski resorts' use of the protein, manufactured under the label SnoMax® (York International, Victor, NY) to initiate snow (ice) crystallization at warmer temperatures; *Ps*INP has also been examined as a candidate for cloud seeding applications as a mechanism of drought relief (Battan, 1969; Morris et al., 2004).

The ability of *Ps*INP to initiate ice nucleation at -2 ˚C seems unremarkable, as water is traditionally assumed to freeze at 0 ˚C. However, a sample of pure water may be supercooled to below -40 ˚C before homogeneous nucleation is observed (Li et al., 2011). Homogeneous nucleation refers to the formation of ice simply by the aggregation of only

water molecules. When an aqueous solution contains some foreign solutes about which water molecules may accumulate (an INP, for example), the potential for heterogeneous nucleation exists. Any ice 'embryo', consisting of a foreign particle surrounded by water molecules, has a conditional critical size. This size must be reached in order for ice crystal growth to continue; below this critical mass, the embryo will disintegrate. At this critical mass, two opposing forces are in equilibrium: (1) any mass increase correlates to an increase in free energy (ΔG) which energetically favors shrinkage of the ice crystal, versus the (2) reduction of the surface free energy (ΔG_F) which is decreased when the embryo grows and the volume to surface area ratio increases (Mazur, 2010). In its capacity as a heterogeneous nucleator, *Ps*INP exceeds this critical mass on its own, bypassing the normal physical restraints applied to small ice embryos.

To date, the tertiary structure of an INP has yet to be experimentally determined, and therefore, the mechanism by which ice formation is induced is poorly understood. Fortunately, advances in protein sequencing and computational modeling techniques may be combined to shed light on the mechanism by which INPs function at the molecular level. A second class of proteins that impacts crystallization of water is comprised of antifreeze proteins (AFPs). AFPs were first discovered in Antarctic fish over 40 years ago and have been identified in several organisms inhabiting environments with persistent subzero temperatures including bacteria, fungi, algae, plants, and arthropods. The molecular mechanisms by which AFPs inhibit ice-formation have been well characterized (DeVries et al., 1969; Gilbert et al., 2004; Hoshino et al., 2003; Janech et al., 2006; Fei et al., 2008; Hawes et al., 2011). Based on their antithetical functions, INPs and AFPs were not expected to be highly similar. However, these two groups of proteins

share a highly conserved, repetitive TXT amino acid motif (threonine followed by any inward pointing amino acid, then another threonine residue) that has been shown to play a crucial role in conferring ice-binding ability (Graether et al., 2000). Figure 1 illustrates threonyl oxygens of an AFP (from the beetle *Tenebrio molitor*) interacting with an aqueous solvent. These oxygen atoms may mimic the structure of oxygens in an ice crystal lattice, encouraging the binding of water molecules (Liou et al., 2000).

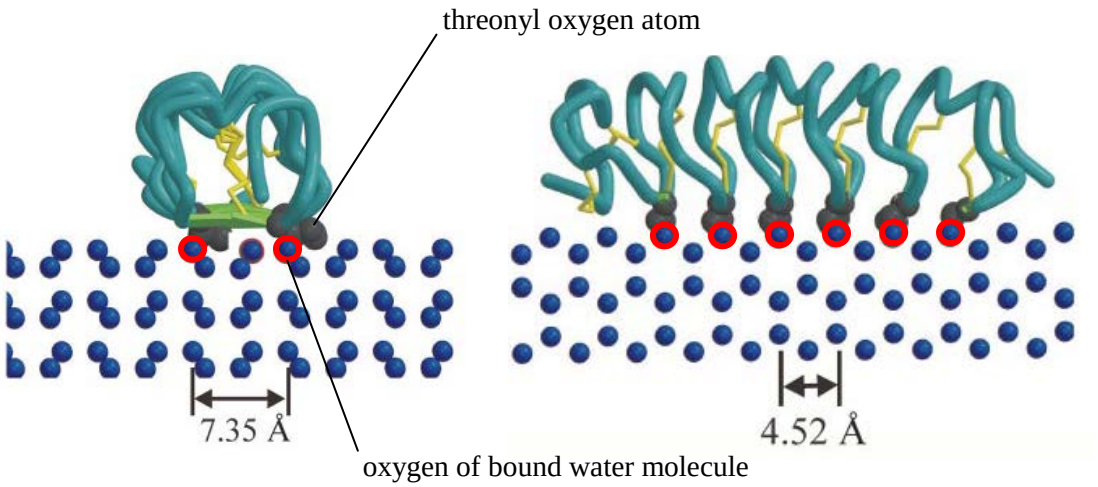

Figure 1. Association of threonyl oxygen atoms of an AFP in aqueous solution with oxygen atoms (outlined in red) of water molecules (adapted from Liou et al., 2000).

It is still poorly understood what specific properties of INPs and AFPs contribute to their highly dissimilar biological functions, given their highly similar associations with water molecules. It has been suggested that the difference in the sheer mass of proteins may be responsible. INPs tend to be at least 10 times larger than AFPs, which could be a reflection of a minimum size requirement for an ice-forming surface with effective nucleation properties. Large INPs provide large surfaces that serve as a foundation for

crystallization, whereas the binding sites of relatively smaller AFPs shield ice nuclei from further aggregation (Graether, 2001). While this seems plausible, the exact source of this phenomenon deserves further investigation.

Intracellular ice formation (IIF) is generally thought to be a lethal event, but the sources of cellular damage associated with IIF are uncertain. There are two popular hypotheses concerning the initiation of IIF: (1) extracellular ice simply propagates through preexisting pores in the cell membrane, initiating IIF, and (2) extracellular ice formation (EIF) is responsible for conformational changes in the structure of the cell membrane, rendering it an effective heterogeneous nucleator for intracellular ice (Mazur et al., 2005; Toner et al. 1993). Independent of the actual mechanism, EIF occurs prior to IIF. As the extracellular medium freezes, the concentration of solutes in the unfrozen portion increases, promoting osmotically driven water flow from within the cell, and the maximum rate of this flow is set by the water permeability of the cell membrane (Mazur, 1963). This basic principle explains the impact of different cooling rates on cell membrane integrity during a freeze-thaw cycle. At very low cooling rates, intracellular water is able to flow out of the cell before IIF occurs, and at very high cooling rates, IIF is complete before any water traverses the cell membrane. Dumont et al. found that samples frozen at rates of 5 °C/min and 30,000 °C/min maintained significantly higher proportions of cells with intact membranes than samples frozen at 180, 250, and 5,000 °C/min (Dumont et al., 2004).

Additionally, studies conducted with the industrial product SnoMax® indicate that the protein, when present in extracellular medium, reduces the chaotic distribution of nucleation in solution and increases cell survival when present at sufficiently high

concentrations (Missous et al., 2007). I hypothesized that intracellular expression of a water-structuring protein, such as *Ps*INP, in combination with a low, highly controlled cooling rate (-1 °C • min^{-1}) will allow for the orderly organization of water molecules during cell freezing, and membrane integrity will be maintained following thawing.

MATERIALS AND METHODS

Sf-21 Cell Maintenance

Sf-21 (*Spodoptera frugiperda*) cells (Invitrogen Corporation, Carlsbad, CA) were cultured in 75 cm^2 cell culture flasks with Sf-900 III media (Invitrogen Corporation, Carlsbad, CA) at 26.5 °C in air. Penicillin (50 U/ml), streptomycin (50 g/ml), and amphotericin B (12.5 µg/ml) (MP Biomedicals, Solon, OH) were added to the Sf-900 III media. Cells were grown to a density of $20 \cdot 10^6$ cells/flask and sub-cultured to $1 \cdot 10^6$ cells per flask weekly.

Subcloning of the *Ps*INP gene

A nucleotide sequence encoding for the central motif of INP from *Pseudomonas syringae* was synthesized (Gene Oracle, Mountain View, CA) and cloned into the pENTR/D-TOPO cloning vector (Invitrogen, Grand Islands, NY) following the protocol provided by the manufacturer. The *Ps*INP sequence was subcloned into the p1B/V-5-HIS-DEST vector for insect cell expression using clonase technology (Invitrogen, Grand Islands, NY).

Transfection of Sf-21 cells

3 million Sf-21 cells were plated in 60 mm dishes at $1.5 \cdot 10^6$ cells/ml in a total volume of 2 ml of Graces insect medium (Invitrogen Corporation, Carlsbad, CA). Cells were transfected using Lipofectamin according to the instructions of the supplier (Invitrogen Corporation, Carlsbad, CA). Stable insertion of the transgene was selected

for by exposing cells to 75 µg/ml of blasticidin for one month (Sf-21-*Ps*INP). After one month, cultures were maintained in 12.5 µg/ml blasticidin (MP Biomedicals, Solon, OH).

Buffer composition

The buffer solution used in each of the following two assays was originally developed as a cell desiccation buffer, designed to increase tolerance of cells to water stress (buffer A). The buffer contains no conventional cryoprotective agents, but is comprised of: 40 ml 0.5 M potassium lactobionate solution per 250 ml buffer solution (35.83 g/200 ml H_2O, pH adjusted to ~7.0 with KOH), MgCl • 6 H_2O (3 mM), taurine (20 mM), HEPES (20 mM), KH_2PO_4 (10 mM), bovine serum albumin (BSA, .25 g/250 ml), and trehalose (200 mM). The pH of the solution was adjusted to 6.8-7.0 with KOH.

Cell incubation assay

Sf-21-*Ps*INP and Sf-21-WT cells were centrifuged at 3,000 • g for 5 minutes, washed with phosphate buffered saline (PBS), centrifuged again, and resuspended to a final density of approximately $1 \cdot 10^6$ cells/ml in buffer A. The cells were then incubated in a water bath at 27 °C for 4 h. A 20 µl sample was withdrawn each hour for cell membrane integrity assessment via trypan blue exclusion assay.

Freeze-thaw assay

Cells were prepared in the same way as described above in buffer A. The resulting cell suspension was aliquoted in 1.0 ml samples into 2.0 ml cryovials (Fisher Scientific, Waltham, MA). Samples were frozen at a controlled rate of -1 °C • min^{-1} using isopropanol in a Nalgene freezing container (Fisher Scientific, Waltham, MA).

Samples remained frozen for at least 24 h at -80 °C, and were rapidly thawed (< 120 seconds) in a 27 °C water bath. Cell membrane integrity was immediately evaluated, again using the trypan blue exclusion assay.

Western Blotting

Sf-21-*Ps*INP cells were washed with 1X PBS and aspirated. Cells were lysed using 100 µl 1X sodium dodecyl sulfate (SDS) sample buffer per sample and transferred to microcentrifuge tubes, containing $1 \cdot 10^6$, $2.5 \cdot 10^6$, and $4.5 \cdot 10^6$ cells. Each cell sample was sonicated for 20 seconds. A 20 µl portion of each sample was then heated to 95 °C for 5 minutes, and loaded onto an SDS polyacrylamide gel (SDS-PAGE gel). A 10 µl quantity of Precision Plus Protein Dual Color Standard (Bio-Rad, Hercules, CA) was loaded into the first lane of the gel. The gel was allowed to run for 30 minutes at 200 V, and proteins were transferred to a nitrocellulose membrane, using a 100 V current for 30 minutes. The membrane was incubated in 25 ml blocking buffer (1X tris-buffered saline (TBS), 0.1% Tween-20, 5% nonfat dry milk) for one hour at room temperature, then subjected to 3 5-minute washes with 15 ml 1X TBS and 0.1% Tween-20 (TBS/T) each. A 1:1000 primary antibody dilution buffer was prepared, comprised of 1X TBS/T, 5% BSA, and 10 µl primary His-tag rabbit antibody (Cell Signaling Technology, Danvers, MA), and the membrane was incubated in this solution on a rocking platform at 4 °C overnight. Following this incubation, the membrane was washed with 15 ml TBS/T for 5 minutes, 3 times. A 1:2000 secondary antibody solution, consisting of 10 ml blocking buffer and 5 µl secondary anti-rabbit IgG antibody (Cell Signaling Technology, Danvers, MA), was applied to the membrane, and incubated on a rocking platform at room temperature for one hour. After 3 5-minute washes with 15 ml TBS/T, proteins were

visualized using a 4-chloro-1-naphthol/3,3′-diaminobenzidine tetrahydrochloride (CN/DAB) substrate kit (Fisher Scientific, Waltham, MA).

Protein modeling

The nucleotide sequence transfected into Sf-21 cells was submitted for computational modeling to the I-TASSER server (Ambrish R et al., 2010; Zhang Y 2008).

Statistical analysis

Results were analyzed using Sigma Plot 11 software. Statistical analyses (ANOVA and student's t-test) were performed on the results, which are reported as mean ± standard error.

RESULTS

To investigate the question of whether intracellular expression of the water-structuring protein *Ps*INP reduces cryogenic injury during cell freezing, the impact of the used freezing buffer (buffer A) on cell viability before the onset of freezing was evaluated. Since transgenic and control cells are exposed to buffer A—which is hyperosmotic and mimics the intracellular ion composition—during freezing, cell membrane integrity was assessed in Sf-21-WT and Sf-21-*Ps*INP cells suspended in buffer A for up to 4 h. Cell membrane integrity declined in a time-dependent manner for Sf-21 and transgenic *Ps*INP-expressing cells (Sf-21-*Ps*INP) incubated at 27 °C. Viability of the two different cell types differed significantly at 1 h and 2 h (n = 6, $p < 0.050$). After 4 h, the proportion of Sf-21-WT cells retaining membrane integrity was 0.42, and for Sf-21-*Ps*INP cells, this proportion was 0.43. With the exception of Sf-21-WT at t(1), all data points significantly differ from t(0) (**Fig. 2**).

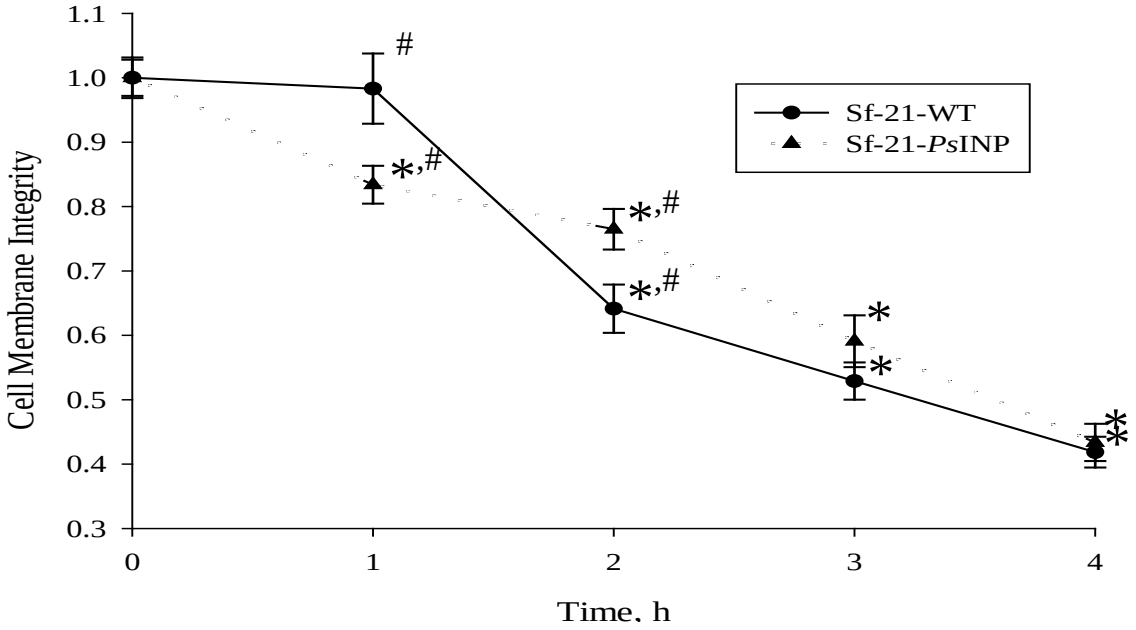

Figure 2. Proportions of cells retaining cell membrane integrity, assessed hourly, for Sf-21-WT and Sf-21-*Ps*INP cells incubated in buffer A at 27 °C for 4 h (n = 6, $p > 0.050$). * denotes statistical significance, relative to t(0). # denotes statistical significance between cell types at a given time point.

After assessing the effect of hyperosmotic stress exerted by buffer A on the two cells types and observing no significant difference between both cell types, a freeze-thaw assay was conducted to investigate the impact of freezing on SF-21-WT and Sf-21-*Ps*INP cell membrane integrity. A significant difference in the amount of cells with intact cell membranes was observed between the two cell types following the freeze-thaw assay ($n = 6$, $p < 0.050$). Sf-21-WT cells retained 60.06% ± 3.25% membrane integrity, while 71.62% ± 3.41% of Sf-21-*Ps*INP cell membranes remained intact (**Fig. 3**).

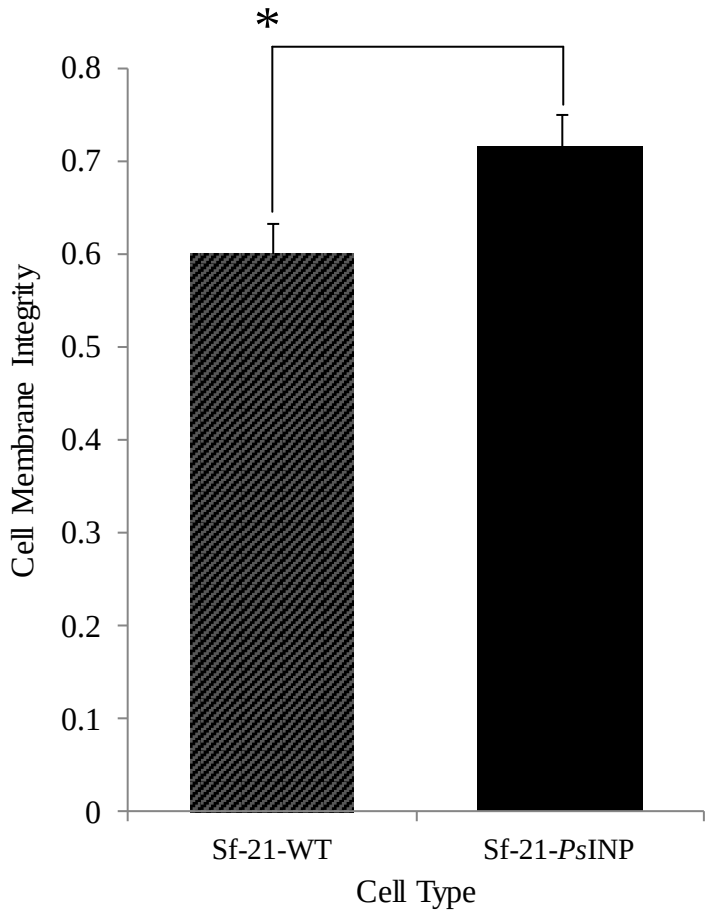

Figure 3. Proportions of Sf-21-WT and Sf-21-*Ps*INP cells retaining membrane integrity following one freeze-thaw cycle ($n = 6$, $p < 0.050$). * denotes statistical significance.

In order to confirm expression of *Ps*INP, Sf-21-*Ps*INP cells were characterized using western blotting techniques. Following this procedure, bands were observed at masses of 77 kD, 90 kD, and 97 kD for samples of 10^6, $2.5 \cdot 10^6$, and $4.5 \cdot 10^6$ cells, respectively (**Fig. 4**).

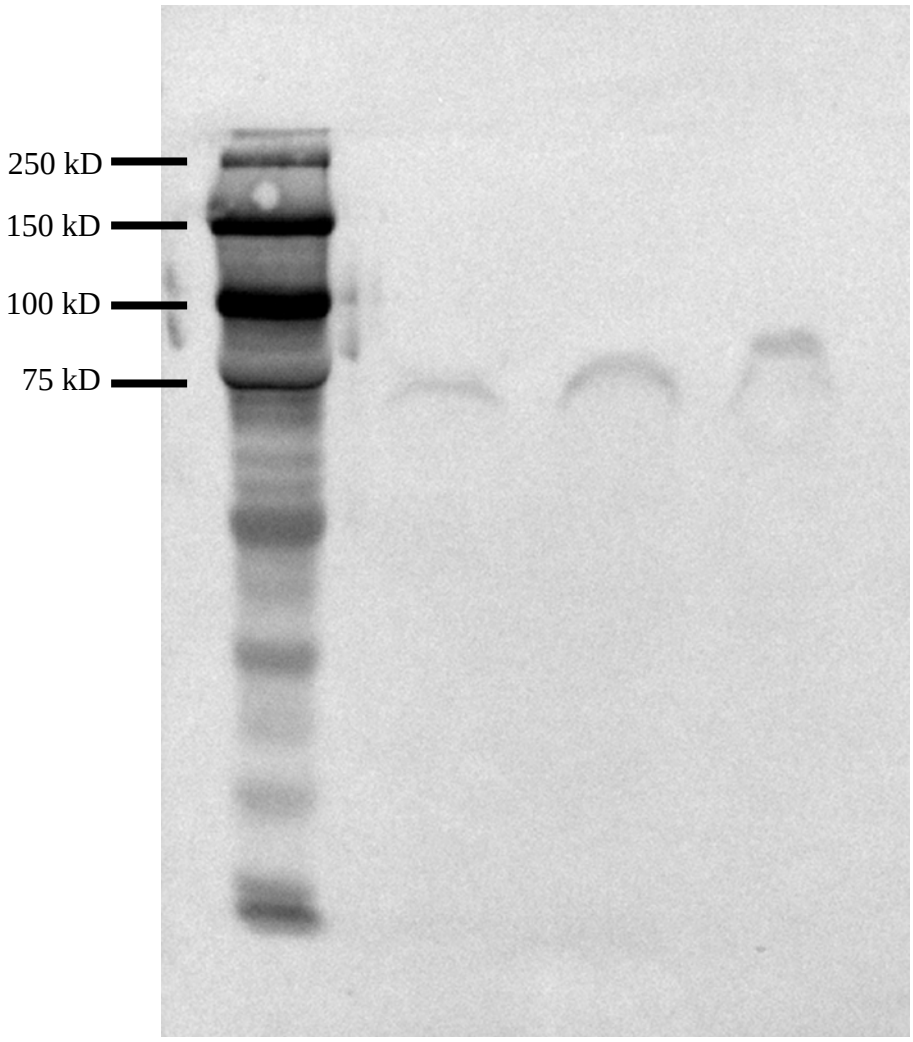

Figure 4. Western blot characterization of protein extracted from Sf-21-*Ps*INP cells. Lanes, from left to right, contained: Precision Plus Protein Dual Color Standard, 10^6, $2.5 \cdot 10^6$, and $4.5 \cdot 10^6$ cells

To investigate the three dimensional structure of *Ps*INP, an *in silico* approach was taken. The *Ps*INP protein model generated on the I-TASSER server is a β-helical structure with a highly repetitive motive sequence (**Fig. 5**) (Ambrish R et al., 2010; Zhang Y 2008). A confidence score (C-score) is assigned to each model produced, within the range of [-5, 2]; increasing C-score corresponds to increasing model confidence. This score is used to determine a template modeling score (TM-score). TM-scores indicate structural similarity between two protein structures, and usually compare some predicted model to a known native structure. Because the exact structure of *Ps*INP is unknown, an algorithm is used to approximate the TM-score based on known correlations between C-scores and TM-scores. A TM-score > 0.5 indicates a model of correct topology. For the *Ps*INP model, the C-score was determined to be -1.60, and the experimental TM-score was 0.52. These values support a high degree of reliability for the generated *Ps*INP model.

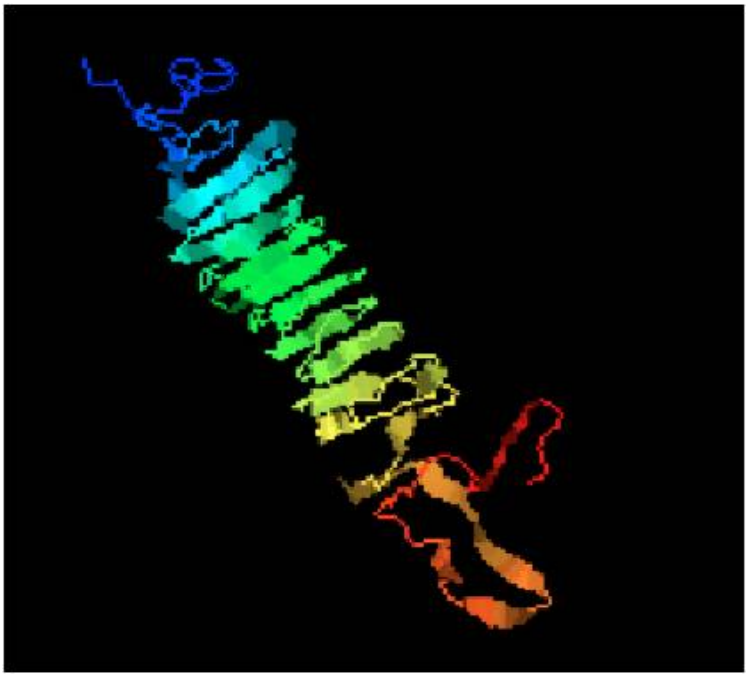

Figure 5. Predicted β-helical tertiary structure of *Ps*INP, generated on the I-TASSER server.

DISCUSSION

The overall goal of this study was to investigate whether the highly repetitive, β-helical, and water-structuring protein *Ps*INP can increase the viability of *Ps*INP-expressing cells following a freeze-thaw cycle. A direct link must be established between *Ps*INP expression and an increase in maintained cell membrane integrity for this hypothesis to be supported. Therefore, it is crucial to ensure that the intracellular presence of *Ps*INP is the only variable contributing to proportions of viable cells observed after freezing and thawing.

The cell incubation assay examined the impact of buffer A—a hyperosmotic environment (~430 mOsM)—on cell membrane integrity, and whether this impact was dependent upon the cell type. Cell membrane integrity was maintained in significntly lower proportions in Sf-21-*Ps*INP cells at 1h and 2h, establishing that *Ps*INP expression does not positively affect cellular responses to the freezing medium prior to ice-nucleation. Therefore, any difference between Sf-21-WT and Sf-21-*Ps*INP cells in retained membrane integrity following a freeze-thaw cycle can be directly attributed to the expression of *Ps*INP. It should be noted that Sf-21-*Ps*INP cells are significantly and negatively impacted by a hyperosmotic environment for the first 2 h, relative to Sf-21-WT cells. This difference may be driven by the function of *Ps*INP as a water-structuring protein; free water molecules within the cell are expected to be bound by *Ps*INP to a minimal degree at temperatures above the ice nucleation temperature. This effect may exaggerate the impact of hyperosmotic extracellular conditions.

This data also provides an estimate of how much the cell membrane integrity may be expected to decline before the samples completely freeze. Prior to freezing, samples

were suspended in buffer A at room temperature (~21 °C) and then cooled to -80 °C at a rate of -1 °C • min^{-1}. The 1.0 ml samples will therefore be completely frozen within one hour, and at this time point, at least ~85% of cell membranes remains intact (the lower value at 1 h was 84.95% ± 3.64% for Sf-21-*Ps*INP cells). For *Ps*INP cells at 1 h, this is a significant decrease, and this may be considered an maximum projection for cell membrane integrity following a freeze-thaw cycle. As 28.38% of Sf-21-*Ps*INP cells lost membrane integrity following complete freezing and thawing, ~50% of this loss is due to hyperosmotic stress and the remaining ~50% is the result of cryoinjury.

The expression of *Ps*INP significantly increases the proportion of cells with intact membranes. This may be due to the repetitive TXT motif, common to all INPs, found within *Ps*INP. In order to determine the exact role these repeats play in conferring cryoprotection to Sf-21-*Ps*INP cells, an additional line of Sf-21 cells could be developed which expresses variant forms of the *Ps*INP gene. Graether et al. carried out a similar study, examining the function of the TXT motif in a spruce budworm AFP by replacing specific threonine residues with leucine (Graether et al., 2000). Substituting leucine molecules (a hydrophobic amino acid) for threonine residues (with a polar neutral side chain) within TXT repeats would allow the proposed influence of threonyl oxygens on the ice nucleation activity of the total protein to be quantified. Cells expressing this modified form of *Ps*INP would be expected to maintain lower proportions of cell membrane integrity. Additionally, solutions of *Ps*INP and its altered counterpart dissolved in buffer A should have significantly different freezing points, with *Ps*INP increasing the freezing point of the solution more effectively than the leucine containing protein.

The predicted molecular weight of *Ps*INP is 26.99 kD, much smaller than the observed Western Blot bands. However, other INPs produced by *P. syringae* are known to aggregate during processing for Western Blotting (Ruggles et al., 1993). The greater the size of an ice nucleator, the higher the nucleation temperature. This effect becomes exaggerated at increasing temperatures; as the nucleation temperature approaches 0 °C, greater nucleator mass is required to affect diminishing increases in nucleation temperature (Burke and Lindow, 1990). The tendency of INPs to form aggregates capable of inciting ice nucleation at elevated temperatures may explain the protein bands with higher than anticipated masses.

The computational model of *Ps*INP is consistent with other models of INPs and AFPs as β-helical structures (Graether et al., 2000; Liou et al., 2000; Graether et al., 2001; Garnham et al., 2011). The reliability of the predicted structure supports the hypothesis that β-sheets within the protein serve as planar surfaces at which water molecules may interact with threonyl oxygens and initiate homogeneous nucleation.

CONCLUSIONS

The major conclusions of this study may be summarized as follows:

(1) Expression of the protein *Ps*INP provided no advantage to cells exposed to a hyperosmotic and intracellular-like environment; in fact, Sf-21-*Ps*INP cells were significantly negatively impacted by these conditions (relative to Sf-21-WT cells) for the first 2 h of incubation.

(2) Sf-21-*Ps*INP cells maintained cell membrane integrity in significantly greater proportions than Sf-21-WT cells, and this difference can be directly attributed to *Ps*INP expression.

(3) Western Blot characterization confirms the transgenic expression of *Ps*INP and also illustrates the tendency of INPs to aggregate.

(4) The computational model generated on the I-TASSER server is consistent with other published models of INPs and AFPs, and with the hypothesis that threonyl residues located in β-sheet regions mediate the initiation of ice nucleation.

LITERATURE CITED

Ambrish, R., Kucukural, A. and Zhang, Y. 2010. I-TASSER: a unified platform for automated protein structure and function prediction. *Nature Protocols*. 5: 725-738.

Battan, L. J. 1969. Harvesting the clouds. Advances in weather modification. Doubleday & Co., Inc., Garden City, New York.

Burke, M. J. and Lindow, S. E. 1990. Surface properties and size of the ice nucleation site in ice nucleation active bacteria: theoretical considerations. *Cryobiology*. 27: 80-84.

DeVries, A. L. and Wohlschlag, D. E. 1969. Freezing resistance in some Antarctic fishes. *Science*. 163: 1073-1075.

Dumont, F., Marechal, P. and Gervais, P. 2004. Cell size and water permeability as determining factors for cell viability after freezing at different cooling rates. *Applied and Environmental Microbiology*. 70: 268-272.

Fei, Y. B., Cao, P. X., Gao, S. Q., Wang, B., Wei, L. B., Zhao, J., Chen, G. and Wang, B. H. 2008. Purification and structure analysis of antifreeze proteins from *Ammopiptanthus mongolicus*. *Preparative Biochemistry and Biotechnology*. 38: 179-190.

Garnham, C. P., Campbell, R. L., Walker, V. K. and Davies, P. L. 2011. Novel dimeric β-helical model of an ice nucleation protein with bridged active sites. *BMC Structural Biology*. 11: 36.

Gilbert, J. A., Hill, P. J., Dodd, C. E. R. and Laybourn-Parry, J. 2004. Demonstration of antifreeze protein activity in Antarctic lake bacteria. *Microbiology*. 150: 171-180.

Govindarajan, A. G. and Lindow, S. E. 1988. Phospholipid requirement for expression of ice nuclei in *Pseudomonas syringae* and *in vitro*. *Journal of Biological Chemistry*. 263: 9333-9338.

Govindarajan, A. G. and Lindow, S. E. 1988. Size of bacterial ice-nucleation sites measured *in situ* by radiation inactivation analysis. *Proc. Natl. Acad. Sci. USA*. 85: 1334-1338.

Graether, S. P., Kuiper, M. J., Gagné, S. M., Walker, V. K., Jia, Z., Sykes, B. D. and Davies, P. L. 2000. B-helix structure and ice-binding properties of a hyperactive antifreeze protein from an insect. *Nature*. 406: 325-328.

Graether, S. P. and Jia, Z. 2001. Modeling *Pseudomonas syringae* ice-nucleation protein as a β-helical protein. *Biophysical Journal*. 80: 1169-1173.

Gurian-Sherman, D. and Lindow, S. E. 1993. Bacterial ice nucleation: significance and molecular basis. *FASEB Journal*. 7: 1338-1343.

Hawes, T. C., Marshall, C. J. and Wharton, D. A. 2011. Antifreeze proteins in the Antarctic springtail, *Gressittacantha terranova*. *Journal of Comparative Physiology B*. 181: 713-719.

Hoshino, T., Kiriaki, M., Ohgiya, S., Fujiwara, M., Kondo, H., Nishimiya, Y., Yumoto, I. and Tsuda, S. 2003. Antifreeze proteins from snow mold fungi. *Canadian Journal of Botany*. 81: 1175-1181.

Janech, M. G., Krell, A., Mock, T., Kang, J. S. and Raymond, J. A. 2006. Ice-binding proteins from sea ice diatoms (Bacillariophyceae). *Journal of Phycology*. 42: 410-416.

Li, T., Donadio, D., Russo, G. and Galli, G. 2011. Homogeneous ice nucleation from supercooled water. *Physical Chemistry Chemical Physics*. 13: 19807-19813.

Liou, Y., Tocilj, A., Davies, P. L. and Jia, Z. 2000. Mimicry of ice structure by surface hydroxyls and water of a β-helix antifreeze protein. *Nature*. 406: 322-324.

Lindow, S. E., Arny, D. C. and Upper, C. D. 1982. Bacterial ice nucleation: a factor in frost injury to plants. *Journal of Plant Physiology*. 70: 1084-1089.

Maki, L. R., Galyan, E. L., Mei-Mon, C. and Caldwell, D. R. 1974. Ice nucleation induced by *Pseudomonas syringae*. *Applied Microbiology*. 28: 456-459.

Mazur, P. 1963. Kinetics of water loss from cells at subzero temperatures and the likelihood of intracellular freezing. *Journal of General Physiology*. 47: 347-369.

Mazur, P., Shinsuke, S., Pinn, I. L., Kleinhans, F. W. and Edashige, K. 2005. Extra- and intracellular ice formation in mouse oocytes. *Cryobiology*. 51: 29-53.

Mazur, P. 2010. A biologist's view of the relevance of thermodynamics and physical chemistry to cryobiology. *Cryobiology*. 60: 4-10.

Missous, G., Thammavongs, B., Dieuleveux, V., Gueguen, M. and Panff, J. M. 2007. Improvement of the cryopreservation of the fungal starter *Geotrichum candidum* by artificial nucleation and temperature downshift control. *Cryobiology*. 55: 66-71.

Morris, C. E., Georgakopoulos, D. G. and Sands, D. C. 2004. Ice nucleation active bacteria and their potential role in precipitation. *Journal de Physique*. 121: 87-103.

Morris, C. E., Kinkel, L. L., Kun, X., Prior, P. and Sands, D. C. 2007. A surprising niche for the plant pathogen *Pseudomonas syringae*. *Infection, Genetics and Evolution*. 7: 84-92.

Morris, C. E., Sands, D. C., Vinatzer, B. A., Glaux, C., Guilbaud, C., Buffiére, A., Yan, S., Cominguea, H. and Thompson, B. M. 2008. The life history of the plant pathogen *Pseudomonas syringae* is linked to the water cycle. *Journal of the International Society for Microbial Ecology*. 2: 321-334.

Morris, C. E., Sands, D. C., Vanneste, J. L., Montarry, J., Oakley, B., Guilbaud, C. and Glaux, C. 2010. Inferring the evolutionary history of the plant pathogen *Pseudomonas syringae* from its biogeography in headwaters of rivers in North America, Europe, and New Zealand. *American Society for Microbiology*.

Mueller, G. M., Wolber, P. K. and Warren, G. J. 1990. Clustering of ice nucleation protein correlates with ice nucleation activity. *Cryobiology*. 27: 416-422.

Ruggles, J. A., Nemecek-Marshall, M. and Fall, R. 1993. Kinetics of appearance and disappearance of classes of bacterial ice nuclei support an aggregation model for ice nucleus assembly. *Journal of Bacteriology*. 175: 7216-7221.

Toner, M., Cravalho, E. G., Stachecki, J., Fitzgerald, T., Tompkins, R. G., Yarmush, M. L. and Armant, D. R. 1993. Nonequilibrium freezing of one-cell mouse embryos: membrane integrity and developmental potential. *Biophysical Journal*. 64: 1908-1921.

Walker, V. K., Palmer, G. R. and Voordouw, G. 2006. Freeze-thaw tolerance and clues to the winter survival of a soil community. *Applied and Environmental Microbiology*. 72: 1784-1792.

Wolber, P. K., Deininger, C.A., Southworth, M.W., Vandekerckhove, J., van Mantagu, M. and Warren, G. J. 1986. Identification and purification of a bacterial ice-nucleation protein. *Proc. Natl. Acad. Sci. USA.* 83: 7256-7260.

Zhang, Y. 2008. I-TASSER: server for protein 3D structure prediction. *BMC Bioinformatics*. 9: 40

APPENDIX A

This research was included in a presentation at the annual meeting of the Biomedical Engineering Society (BMES) in Atlanta, GA, October 24-27, 2012 (see next page).

Intracellular Ice Nucleation Protein Reduces Cryogenic Injury in Eukaryotic Cells

Avril Harder[1], Dilini A. Samarajeewa[1], Mehmet Toner[2], Nilay Chakraborty[3], and Michael A. Menze[1].
[1]Dept. of Biological Sciences, Eastern Illinois University, Charleston, IL, 61920. [2]Center for Engineering in Medicine, Harvard Medical School, Boston, MA, 02114. [3]Dept. of Mechanical Engineering, University of Michigan, Dearborn, MI, 48128. amharder@eiu.edu

Abstract

Exposure of isolated eukaryotic cells to subzero temperatures typically leads to a significant or complete loss of plasma membrane integrity and cell viability. One of the primary reasons for this loss of cell viability can be attributed to the formation of lethal intracellular ice at supercooled temperatures (below the freezing point of ice). In this study we hypothesized that slow and regulated formation of intracellular ice at temperatures above the ice crystallization temperature (without significant supercooling) will diminish injury to eukaryotic cells. Under certain conditions the bacterium *Pseudomonas syringae* synthesizes an extracellular ice nucleation protein (INP) (Swiss-Prot: O30611), which is capable of promoting ice formation at warmer temperatures (above the spontaneous ice formation temperature of pure water). INPs serve as organization platforms in the orderly formation of water structure during freezing. We designed a protein of 530 amino acids (*Ps*INP) based on multiples of the amino acid motive SSLTAGYGSTQTAQ derived from the highly repetitive central domain of the protein O30611. PsINP was expressed in *Escherichia coli* and purified using affinity chromatography. Addition of purified *Ps*INP to buffer solutions at a concentration of 0.075 mg/ml substantially raised the ice nucleation temperature of the solution. *Ps*INP was then transgenically expressed in cells derived from *Spodoptera frugiperda* (Sf-21) or hepatocellular carcinoma (HepG2). After freezing at 1 °C • min^{-1}, *Ps*INP expressing Sf-21 cells showed an increase in membrane integrity compared to control cells (60.01 ± 3.3% control vs. 71.6 ± 3.4% Sf-21-PsINP; n = 6; ±SE). Furthermore, standard cryomicroscopy demonstrated that HepG2 cells expressing a green fluorescent protein labeled variant of *Ps*INP (HepG2-PsINP-GFP) showed intracellular ice formation at higher temperature than control cells (ΔT = 17.63 ± 1.16 °C; n = 3; ±SE). Our results suggest that induction of orderly intracellular ice formation can reduce cell injury during freezing.

I. Introduction

The bacterium *Pseudomonas syringae* expresses on the outside of the plasma membrane an ice nucleation protein (INP), that efficiently catalyzes ice formation at temperatures as warm as -2 °C [1]. INPs increase the freezing temperature of water and recently the mechanism by which the INP from *P. syringae* structures water (inaK) has been elucidated in more detail [2]. The epiphytic pathogen, *P. syringae*, may use INPs to induce frost damage to plant tissues, gaining access to stored nutrients, and as a means of dispersal via the water cycle [3, 4]. *Ps*INP is a water-structuring protein that aids in the orderly organization of water molecules during freezing. Intracellular ice formation (IIF) is considered to be lethal, which makes INPs unlikely candidates for applications in cryopreservation. However, extracellular ice formation (which precedes IIF) may be even more damaging to cells, causing an increase in solute concentration outside the cell and ultimately cell dehydration, membrane damage, and protein denaturation [5]. Slow, thermally regulated formation of intracellular ice has been shown to be less damaging to cells than crystallization occurring at a faster rate. Cells frozen at low cooling rates (-5 °C/min) remain viable in much larger proportions than cells at intermediate freezing rates (-100-1000 °C/min) [6]. Furthermore, when added to a cellular suspension, a commercially available INP (Snomax®) reduced the time required for freezing to be complete and decreased the chaotic distribution of ice nucleation [7]. Another compound with great potential in cryopreservation is the non-reducing disaccharide trehalose which accumulates in some organisms before the onset of freezing or drying [8]. We hypothesized that:

Intracellular expression of *Ps*INP in eukaryotic cells will promote orderly ice formation and increase viability after cryopreservation in trehalose containing medium.

II. Materials and Methods

A. Freezing and viability assays

Sf-21-*Ps*INP and Sf-21-WT cells were pelleted at 3,000 · g for 5 min, and resuspended to a final density of approximately 1 · 10^6 cells ml^{-1} in buffer containing 200 mM trehalose. The cells were then incubated at 27 °C for 4h. (Nalgene, Rochester, NY). Samples for cryopreservation were frozen at -1 °C/min using an isopropanol based controlled rate freezer. After storage for 24h at -80 °C samples were rapidly thawed (< 120 seconds) in a 27 °C water bath and membrane integrity was evaluated, by trypan blue exclusion assay.

B. Transfection of Sf-21 and HepG2 cells

A nucleotide sequence encoding for the central motive of INP from *P. syringae* was synthesized (Gene Oracle, Mountain View, CA), subcloned into insect and mammalian cell expression vectors, and transfected using Lipofectamin according to the instructions of the supplier (Invitrogen, Grand Island, NY).

II. Materials and Methods (cont'd)

C. Protein modeling

The *Ps*INP sequence was submitted to the I-TASSER server for computational modeling and structure prediction.

D. Cryomicroscopy studies

Purified *Ps*INP (0.075mg/ml) was dissolved in 40 mM HEPES buffer, and 25 µL of the sample was loaded on a glass slide and placed on the Linkam stage for cryomicroscopic observation. The sample was subjected to a decreasing temperature ramp at -10 °C/min while being continuously observed on an upright microscope using a 10x objective. Micrographs were collected at regular interval while subjecting the solution to different temperatures. Ice formation was confirmed using visual inspection (darkening of the image field).

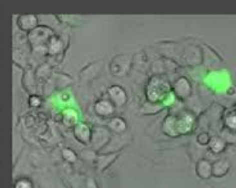

Figure 1. Fluorescence micrograph of HepG2 cells transfected with GFP-labeled *Ps*INP.

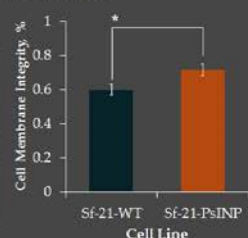

Figure 2. Cell membrane integrity after one freeze-thaw cycle (Sf-21-WT and Sf-21-*Ps*INP cells) in trehalose containing buffer. Viability was significantly higher in cells expressing *Ps*INP.

III. Results

- Transgenic expression of *Ps*INP-GFP was confirmed by fluorescence microscopy in HepG2 cells (Fig. 1) and via Western Blotting in Sf-21 cells for unlabeled *Ps*INP (data not shown).
- Sf-21-WT and Sf-21-*Ps*INP after freezing and thawing showed a significant difference in membrane integrity (Fig. 2). Sf-21-WT cells retained, on average, 60.06 ± 3.25% cell membrane integrity, while 71.62 ± 3.41% of Sf-21-*Ps*INP cell membranes remained intact (n = 6, $p < 0.050$).
- Sf-21-WT and Sf-21-*Ps*INP cells incubated at 27 °C exhibited a decline in cell membrane integrity over time. No significant difference between transgenic and control cells was observed ($p > 0.05$, n = 6). Retention of cell membrane integrity for Sf-21-WT cells was 41.86 ± 2.39%, and for Sf-21-PsINP cells, this proportion was 43.37 ± 2.90% (Fig. 3).
- Cryomicroscopy demonstrates that the addition of *Ps*INP to HEPES buffer substantially increased the ice nucleation temperature of the solution (Fig. 4).

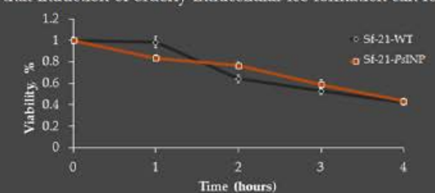

Figure 3. Sf-21-WT and Sf-21-*Ps*INP-expressing cells incubated at 27 °C for 4h. Membrane integrity did not differ significantly at any point between both cell lines.

IV. Discussion

- Long term incubation at 27 °C demonstrates that *Ps*INP expressing cells and control cells do not differ significantly in membrane integrity as a response to the trehalose containing preservation medium prior to freezing.
- The difference in cell viability between the two cell types observed after one freezing-thawing cycle is attributed to the presence or absence of *Ps*INP.
- Threonyl oxygens in the internal repetitive region of *Ps*INP most likely align with oxygen atoms in water molecules of the ice crystal lattice, providing an effective nucleation-inducing surface on the predicted β-sheet regions of the protein (Fig. 5) [9].

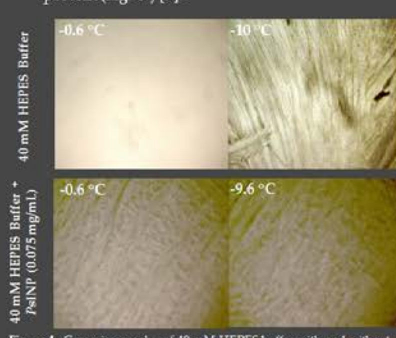

Figure 4. Cryomicrographs of 40 mM HEPES buffer with and without *Ps*INP (0.075 mg/mL) at -0.6 °C and -10 °C/-9.6 °C, respectively.

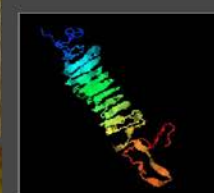

Figure 5. Predicted tertiary structure of *Ps*INP, modeled on the I-TASSER server. β-sheet regions likely serve as ice nucleation surfaces.

V. References

1. Gurian-Sherman, D. and Lindow, S. E. 1993. Bacterial ice nucleation: significance and molecular basis. FASEB Journal. 7: 1338-1343.
2. Graether, S.P. and Z. Jia. 2001. Modeling *Pseudomonas syringae* ice-nucleation protein as a β-helical protein. Biophysical Journal. 80: 1169-1173.
3. Lindow, S. E., Arny, D. C. and Upper, C. D. 1982. Bacterial ice nucleation: a factor in frost injury to plants. Journal of Plant Physiology. 70: 1084-1089.
4. Morris, C. E., Sands, D. C., Vinatzer, B. A., Glaux, C., Guilbaud, C., Buffière, A., Yan, S., Dominguez, H. and Thompson, B. M. 2008. The life history of the plant pathogen *Pseudomonas syringae* is linked to the water cycle. Journal of the International Society for Microbial Ecology. 2: 321-334.
5. Walker, V. K., Palmer, G. R. and Voordouw, G. 2006. Freeze-thaw tolerance and clues to the winter survival of a soil community. Applied and Environmental Microbiology. 72: 1784-1792.
6. Dumont, F., Marechal, P. and Gervais, P. 2004. Cell size and water permeability as determining factors for cell viability after freezing at different cooling rates. Applied and Environmental Microbiology. 70: 268-272.
7. Missous, G., Thammavongs, B., Dieuleveux, V., Guegen, M. and Panoff, J. M. 2007. Improvement of the cryopreservation of the fungal starter Geotrichum candidum by artificial nucleation and temperature downshift control. Cryobiology. 55: 66-71.
8. Westh, P. and H. Ramløv. 1991. Trehalose accumulation in the tardigrade *Adorybiotus coronifer* during anhydrobiosis. Journal of Experimental Zoology. 258: 303-311.
9. Liou, Y., Tocilj, A., Davies, P.L. and Jia, Z. 2000. Mimicry of ice structure by surface hydroxyls and water of a β-helix antifreeze protein. Nature. 406: 322-324.